

The $\pm 45^\circ$ Correlation Interferometer as a Means to Measure Phase Noise of Parametric Origin

Enrico Rubiola, Vincent Giordano, and Hermann Stoll

Abstract—A radiofrequency interferometric detector is combined with the correlation-and-averaging technique in a new scheme for the measurement of the phase noise of a component. The method relies upon the assumption that the phase noise of the component being tested (DUT) exceeds the amplitude noise, which is consistent with the general experience in the field of wireless engineering. The new scheme is based on the amplification of the DUT noise sidebands and on the simultaneous measurement of the amplified noise by means of two mixers driven in quadrature, $\pm 45^\circ$ off the carrier phase. The $\pm 45^\circ$ detection has two relevant properties, namely 1) the sensitivity is neither limited by the thermal energy $k_B T_0$, nor by temperature uniformity, and 2) the noise of the measurement amplifier is rejected, despite a single amplifier being shared by the two channels of the correlator. The article provides the theoretical background and experimental results. The sensitivity of the first 100-MHz prototype, given in terms of the $S_\phi(f)$ floor, is some 12 dB below $k_B T/P_0$, where P_0 is the carrier power. Using a dual carrier suppression scheme, the residual flicker is as low as -168 dBrad²/Hz at $f = 1$ Hz off the carrier.

Index Terms—AM noise, correlation, noise measurement, phase noise, random noise.

I. INTRODUCTION

WHEN a sinusoidal signal of frequency ν_0 crosses a two-port component, the latter contributes its internal noise to the output signal $s(t)$. The usual representation of $s(t)$ is

$$s(t) = \sqrt{2R_0 P_0} [1 + \alpha(t)] \cos[2\pi\nu_0 t + \phi(t)] \quad (1)$$

where P_0 is the DUT output power and R_0 is the characteristic impedance; $\alpha(t)$ and $\phi(t)$ are the random variables that represent amplitude (AM) and phase (PM) noise, respectively. The physical quantity of major interest is $S_\phi(f)$, i.e. the power spectrum density (PSD) of $\phi(t)$.

For our purposes, $s(t)$ is best described as

$$s(t) = \sqrt{2R_0 P_0} \cos(2\pi\nu_0 t) + n_c(t) \cos(2\pi\nu_0 t) - n_s(t) \sin(2\pi\nu_0 t) \quad (2)$$

Manuscript received July 1, 2001; revised December 4, 2002.

E. Rubiola is with the Ecole Supérieure de Sciences et Technologies de l'Ingénieur de Nancy (ESSTIN)—Laboratory of Physics of Ionized Media and Applications (LPMIA), Université Henri Poincaré, Nancy, France (e-mail: rubiola@esstin.uhp-nancy.fr).

V. Giordano is with the Laboratoire de Physique et de Métrologie des Oscillateurs (LPMO)—CNRS, Besançon, France (e-mail: giordano@lpmo.edu).

H. Stoll is with the Max-Planck-Institut für Metallforschung, Stuttgart, Germany (e-mail: stoll@mf.mpg.de).

Digital Object Identifier 10.1109/TIM.2003.809472

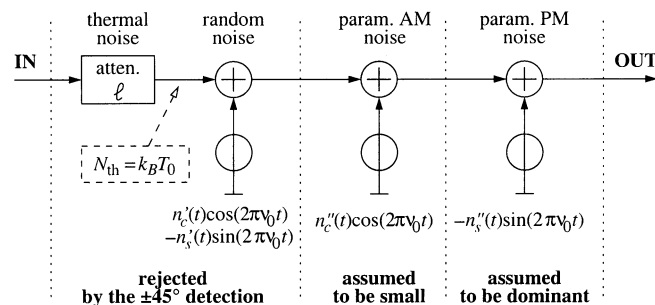
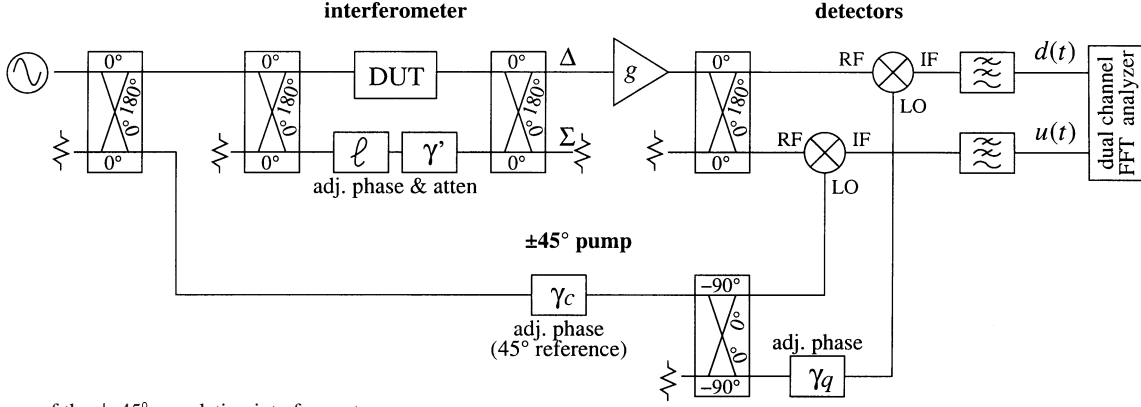


Fig. 1. Noise model of a passive DUT.

which is equivalent to (1) under the assumption of high signal-to-noise ratio, i.e., $\overline{n_c^2} + \overline{n_s^2} \ll 2R_0 P_0$; often, $n_c(t)$ and $n_s(t)$ are named *in-phase* and *quadrature* components of noise. It holds that $\alpha(t) = n_c(t)/\sqrt{2R_0 P_0}$ and $\phi(t) = n_s(t)/\sqrt{2R_0 P_0}$, which is easily seen from the vector representation of (2).

The interferometric measurement consists of suppressing the $\sqrt{2R_0 P_0} \cos(2\pi\nu_0 t)$ term in (2), and of detecting the noise terms. Searching back through the bibliography, the interferometric carrier suppression was used in the late sixties to enhance the dynamic range of spectrum analyzers [1], and to measure the phase noise of pulsed power amplifiers [2]. The amplification of the noise sidebands was introduced later [3], while further improvements are reported in the references [4], [5]. The $\pm 45^\circ$ correlation scheme was proposed for the measurement of the near-dc $1/f$ fluctuations of resistance in thin metal films [6].

The phase noise measurement with the $\pm 45^\circ$ scheme relies upon two assumptions on the parametric noise of the DUT, namely 1) PM and AM noise types are independent, and 2) PM noise is dominant as compared to the AM noise. Fig. 1 details the DUT model, emphasizing the logic division between parametric and random noise; this model, chiefly inspired to passive devices, can be adapted to the active ones. The overall thermal noise is $k_B T_0/\ell + k_B T_{\text{DUT}}(\ell - 1)/\ell$ in the general case, or $k_B T_0$ if the DUT temperature is equal to the room temperature T_0 . The in-phase and quadrature components of thermal noise are independent processes with identical statistical properties. Random noise is similar to thermal noise, to the extent that the in-phase and quadrature components are independent and have equal statistical properties. Conversely, the parametric noise of actual devices consists of a set of independent processes, each of which tends to modulate either a resistance or a capacitance, thus to produce in-phase or quadrature noise rather than some combination of both. Accordingly, the model contains pure AM and PM noise sources, without a cross term. General experience

Fig. 2. Scheme of the $\pm 45^\circ$ correlation interferometer.

indicates that in radiofrequency devices the reactance fluctuations have more effect than the fluctuations of resistance, and, therefore, the dominant noise is of the PM type, while this hypothesis must be reversed at low carrier frequencies, i.e., audio and below. Of course, the physical analysis of the specific device type is always needed.

II. BASICS OF THE NOISE DETECTION METHOD

The scheme of the proposed instrument is shown in Fig. 2. Setting the variable attenuation ℓ and the variable phase shift γ' equal to the DUT phase and attenuation, the carrier is suppressed at the Δ output of the hybrid coupler. The suppression mechanism has no effect on the DUT noise, which is amplified and down converted to baseband by the mixers. The interferometer is similar to an ac impedance bridge [7], [8], but it is used to measure the noise of a device through the fluctuations of the null signal instead of measuring a constant impedance. The detection system is a variation of the lock-in amplifier [9], optimized for low-noise RF measurements.

Let us first analyze the scheme of Fig. 2 in a simplified case, accounting for the DUT noise only as the signal to be detected, and removing all the other noise sources. The signal at the RF input of the mixers is

$$x_{\text{RF}} = \sqrt{\frac{g}{4\ell_h^2}} [n_c(t) \cos(2\pi\nu_0 t) - n_s(t) \sin(2\pi\nu_0 t)] \quad (3)$$

where g is the gain of the amplifier, ℓ_h is the dissipative loss of the hybrids, supposed equal, and the factor 4 accounts for the intrinsic loss of the two hybrids along the signal path. Owing to the circuit topology, the mixer pump signals are of the form $\cos(2\pi\nu_0 t \pm \pi/4)$. Thus, filtering out the $2\nu_0$ terms, the signals at the input of the fast Fourier transform (FFT) analyzer are

$$u(t) = \sqrt{\frac{g}{4\ell_h^2 \ell_m}} [n_c(t) + n_s(t)] \quad (4)$$

$$d(t) = \sqrt{\frac{g}{4\ell_h^2 \ell_m}} [n_c(t) - n_s(t)] \quad (5)$$

where ℓ_m is the SSB loss of the mixer, as usually defined in the data sheet of actual components.

A vector representation of phase and amplitude noise, and of their detection with the $\pm 45^\circ$ scheme, is shown in Fig. 3. The $\pm 45^\circ$ detection is similar to the FM stereo broadcastings, and to

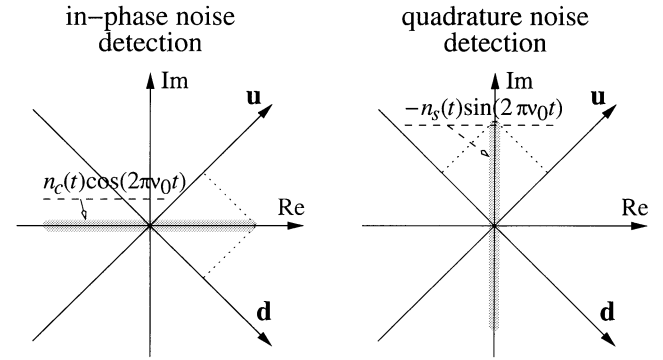


Fig. 3. Vector representation of phase and amplitude noise on the complex plane, and of the noise detection by scalar projection on the \mathbf{u} and \mathbf{d} axes. As $n_c(t)$ and $n_s(t)$ are random variables, we can only represent the segment swept by the corresponding vectors, which is shown as the shadowed areas.

the PAL television standard [10], where the transmitted signals are $L \pm R$ (left±right) and $Y \pm C$ (chrominance±luminance). L and R , as well as Y and C , can be regarded as a pair of independent random signals whose sum and difference define a pair of $\pm 45^\circ$ axes.

As $u(t)$ and $d(t)$ are power-type signals, the correlation function is defined as

$$\mathcal{R}_{ud}(\tau) = \lim_{\theta \rightarrow \infty} \frac{1}{\theta} \int_0^\theta u(t) d^*(t-\tau) dt. \quad (6)$$

The symbol “*” stands for complex conjugate and can be omitted because $n_c(t)$ and $n_s(t)$, and consequently $u(t)$ and $d(t)$, are real signals. Substituting (4) and (5) into (6), the latter turns into

$$\mathcal{R}_{ud}(\tau) = \frac{g}{4\ell_h^2 \ell_m} [\mathcal{R}_{n_c}(\tau) - \mathcal{R}_{n_s}(\tau)]. \quad (7)$$

This occurs because $n_c(t)$ and $n_s(t)$ are independent and, therefore, $\mathcal{R}_{n_c n_s}(\tau) = \mathcal{R}_{n_s n_c}^*(\tau) = 0$. The cross PSD of $u(t)$ and $d(t)$, that is the Fourier transform

$$S_{ud}(f) = \int_{-\infty}^{\infty} \mathcal{R}_{ud}(\tau) \exp(-2\pi j f \tau) d\tau \quad (8)$$

of $\mathcal{R}_{ud}(\tau)$, is equal to the difference

$$S_{ud}(f) = \frac{g}{4\ell_h^2 \ell_m} [S_{n_c}(f) - S_{n_s}(f)] \quad (9)$$

of the two individual PSDs. Reintroducing $\alpha(t)$ and $\phi(t)$, under the assumption that PM noise is dominant with respect to AM noise, (9) becomes

$$S_{ud}(f) = \frac{R_0 P_0 g}{4\ell_h^2 \ell_m} [S_\alpha(f) - S_\phi(f)] \quad (10)$$

$$\simeq -\frac{R_0 P_0 g}{4\ell_h^2 \ell_m} S_\phi(f). \quad (11)$$

Finally, we can calculate the white noise of the instrument in single-arm mode, as it appears when the DUT is bypassed. Denoting with F the amplifier noise figure, the noise at the amplifier input is $Fk_B T_0$. Thus, the output PSD is $S_{u0}(f) = S_{d0}(f) = gFk_B T_0 R_0 / \ell_h \ell_m$, which corresponds to a single-arm phase noise floor $S_{\phi 0}(f) = 4\ell_h F k_B T_0 / P_0$.

III. NOISE CANCELLATION MECHANISM

Now we carry on the complete noise analysis of Fig. 2. Noise is assumed to be stationary and ergodic, which means that measurements are repeatable, and that the time functions $\alpha(t)$ and $\phi(t)$ are representative of the corresponding processes. Furthermore, all the noise sources following the amplifier are supposed to be negligible. True random noise is not biased by the phase of the carrier. This means that the corresponding $n_c(t)$ and $n_s(t)$ are uncorrelated random functions with equal PSD, which is known since the early studies on noise [11]. As a consequence, this type of noise vanishes in the detection equation (9). This applies to:

- thermal noise, that is clearly unbiased. This type of noise derives from the DUT, from the dissipative loss of the interferometer, and from the resistive termination connected at the lower left port of the interferometer.
- the nonthermal additive random noise of the DUT, that is, by definition, unbiased.
- the equivalent noise $(F - 1)k_B T_0$ of the amplifier. This noise source—not represented in Fig. 1—is equivalent to a random generator of PSD equal to $2\ell_h(F - 1)k_B T_0$, referred to the DUT output. If the residual carrier power at the amplifier input is made sufficiently small by accurate adjustment of the interferometer, the internal noise of the amplifier can not be biased by the phase of the carrier, and therefore it is rejected. In fact, the parametric noise of the amplifier derives from close-to-dc noise up converted by carrier-driven nonlinearity, and the high linearity that derives from small signal operation is sufficient to prevent the up-conversion phenomenon from taking place.

In this condition, the residual *random* noise is only limited by the single-arm noise divided by $\sqrt{2m}$, where m is the number of averaged spectra. Of course, the *parametric* noise remains, which is what we want to measure. Under the assumption that AM noise is negligible with respect to PM noise, (11) holds, and the machine measures the phase noise $S_\phi(f)$ of the DUT.

The $\pm 45^\circ$ detection scheme shows two relevant advantages as compared to the traditional correlation detection, like that of the Allred radiometer [12] and the double interferometer [13]. The first one is that isolation between the two low-noise amplifiers is a critical issue in the other instruments, while this

problem is absent in the proposed circuit that has only one amplifier. The second advantage is that the residual noise of the radiometer and of the double interferometer derives from a temperature difference, and, therefore, the thermal noise compensation relies upon temperature uniformity; conversely, the noise rejection of the proposed scheme derives from the intrinsic properties of the $\pm 45^\circ$ detection scheme, and it is independent of temperature distribution.

Actually, the instrument noise is limited by the noise of the interferometer, which is due to the variable attenuator and phase shifter responsible for the carrier suppression, and by the accuracy of the quadrature condition between the two detectors. Furthermore, the interferometer acts as a discriminator whose correlation time is the group delay difference between the two arms, which causes a fraction of the oscillator noise to be taken in. While the case of small delay DUTs can often be considered ideal, measuring high Q resonators the phase fluctuations of the DUT can not be divided from the oscillator noise, for the measurement of a single resonator relies upon the oscillator stability. Often, it is a good practice to insert two equal resonators in the interferometer, one in each arm, for the correlation time derives from the Q mismatch instead of the Q factor of a single resonator. Obviously, both resonators contribute the detected noise.

IV. IMPLEMENTATION AND RESULTS

The prototype we experimented on works at the carrier frequency $\nu_0 = 100$ MHz. The amplifier shows a gain $g = 41.5$ dB and a noise figure $F \simeq 1.5$ dB. The hybrid losses are $\ell_{h1} = 1$ dB at the DUT output and $\ell_{h2} = 0.4$ dB at the amplifier output, and the SSB loss of the mixers is $\ell_m = 5.5$ dB. All the design follows the rules given in [5].

The reported experiments are made with a carrier power $P_0 = 4$ dBm at the DUT output. In this condition, the residual carrier never exceeds -20 dBm at the amplifier output, which is some 35 dB below the 1-dB saturation level.

The adjustment and calibration procedure is straightforward. The interferometer is first removed, and the amplifier is driven by a synthesizer set to a frequency ν_s of some kilohertz off the carrier frequency ν_0 , and to a low output power P_s (of the order of -80 dBm in our case). This results in a beat note of frequency $f_s = \nu_s - \nu_0$ and rms voltage $V_u = V_d = \sqrt{gP_s R_0 / 2\ell_s \ell_m}$ at the two outputs. In this condition, the output amplitudes are independent of the phase relationship between the two detectors; thus, measuring V_u and V_d we are able to evaluate the SSB gain $V^2/P_s = V_u V_d / P_s = gR_0 / 2\ell_s \ell_m$ of the instrument. The quadrature condition of the two outputs is set acting on γ_q and observing the output cross PSD with the amplifier driven by the synthesizer. As $S_{ud}(f_s)$ is imaginary when the two detectors are in quadrature, γ_q must be adjusted for $\Re\{S_{ud}(f_s)\} = 0$, which takes the high accuracy benefit of a null method. Alternatively, the quadrature condition can be adjusted with higher accuracy by means of a lock-in amplifier, which also turns into easier manual operation; this is due to the faster response and to the analog readout of this type of instrument. Then, the synthesizer is removed and the interferometer restored. A phase modulator, calibrated by means of a network analyzer, is inserted as the

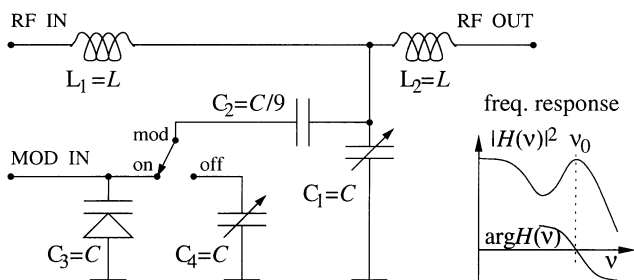


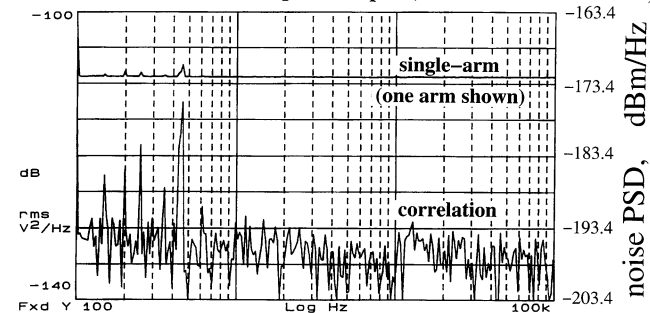
Fig. 4. Low-noise phase modulator.

DUT. Subsequently, the common phase γ_c must be set for the two detectors to be at $\pm 45^\circ$ off the carrier phase. This is accomplished by provisionally setting the machine for arm u to detect PM and arm d AM, which is observed as a null of $d(t)$ in the presence of a phase modulation, and then by replacing the cable in series to γ_c with a calibrated one 45° longer. Finally, the phase-to-voltage gain $k_\phi = \sqrt{S_{ud}(f)/S_\phi(f)}$ is measured by injecting a phase modulation $S_\phi(f)$ and by measuring the corresponding output PSD. It should be observed that the SSB gain V^2/P_s and k_ϕ give the same information, and hence, one measurement could be omitted; nevertheless, we recommend to make both the measurements and to check the result consistency. The gain of our prototype, taken with $P_0 = 4$ dBm, is of 60.4 dBV/rad, with an asymmetry of some ± 0.2 dB between the two arms. This includes two 40-dB low-noise amplifiers, not shown in Fig. 2, inserted between the mixers and the FFT analyzer.

A phase modulator, shown in Fig. 4, has been developed for this type of application. This scheme turned out to be a fortunate choice because of its low internal noise and its suitability to the generation of small-angle modulation, well below $k_B T_0/P_0$. The ripple of the low-pass transfer function is exploited to operate the circuit as a loose bandpass filter ($Q \approx 3$) at the frequency of the right peak, that is made equal to ν_0 . The $C_1 C_2 C_3$ network is a sort of electrostatic lever, in which a change $\Delta C/C$ of the varactor capacitance contributes with some $10^{-2} \Delta C/C$ to C_1 , and, therefore, with $-5 \times 10^{-3} \Delta C/C$ to the resonant frequency. Amplitude is unaffected because the module of the transfer function is locally even around ν_0 , while a small phase change $2Q \Delta C/C \times 5 \times 10^{-3}$ rad takes place. The reactance noise of the varactor is attenuated in the same way, or eliminated by switching the modulation off. Our prototype shows a voltage-to-phase gain of -46 dBrad/V, including the $C(V)$ function of the varactor, and a loss of 0.5 dB.

The measurement uncertainty is chiefly the uncertainty of the network analyzer with which the phase modulator is calibrated; it can be of the order of 0.3–0.5 dB, depending on the available instrument. The measurement of k_ϕ with the transfer function capability of the FFT analyzer, or with a lock-in amplifier, yields a small additional uncertainty, negligible as compared to that of the network analyzer. The quadrature condition between the u and d axes causes negligible uncertainty because it relies upon a null measurement. An error $\delta\gamma_c$ (rad) in the 45° rotation of the ud frame causes a relative error $2(\delta\gamma_c)^2$ in the measurement of ϕ , which is a second-order effect. Additional uncertainty derives from data smoothing, which depends on the number of averaged spectra, and ultimately upon the measurement time.

Equivalent noise at the amplifier input (without interferometer)



Phase noise at the DUT output (interferometer restored)

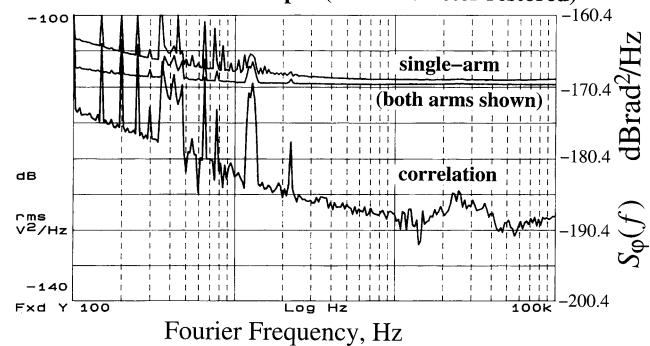


Fig. 5. Residual noise of the instrument, in the absence of the DUT.

Fig. 5 shows the residual noise of the instrument, measured in the absence of the DUT. The upper part of that figure refers to the first part of the experiment, in which the interferometer is removed and the amplifier input is terminated to a resistor. The left vertical scale gives the bare reading of the FFT analyzer, in dBV^2/Hz , while the right scale reports the noise PSD referred to the DUT output. Of course, the difference between the two scales is the DSB gain of the instrument. The single-arm noise is of some -172.5 dBm/Hz, which is consistent with the amplifier noise figure $F \approx 1.5$ dB. The absence of flicker, evident in the left part of the figure, is due to the absence of a carrier signal. The cross PSD reveals a noise reduction of 22 dB, which is of the same order of the limit imposed by the averaging capability ($m = 32767$) of the FFT analyzer. The noise floor is of some 20 dB below the thermal energy $k_B T_0$ at the amplifier input, and it is expected to further decrease if the number of averages is increased. The lower part of Fig. 5 reports the results of the second part of the experiment, in which the interferometer is restored and the DUT is replaced with a short cable. The residual noise $S_\phi(f)$ of the instrument can be read on the right scale. For comparison, the left scale reports the PSD of the output voltage, which is consistent with the upper part of the figure. The single-arm noise reveals the presence of flicker around $f = 100$ Hz, and some asymmetry between the two arms. The single-arm white noise is the same as observed in the absence of the interferometer. The cross PSD reveals the presence of flicker $S_\phi \approx -174$ dBrad²/Hz at $f = 100$ Hz, which is thought to be due to the interferometer. A stray signal of unknown origin is present in the 15 to 40 kHz region. For $f > 7$ kHz, and depending on frequency, the residual noise of the instrument is of some -188 to -190 dBrad²/Hz, which is 10 to 12 dB lower than $k_B T/P_0$.

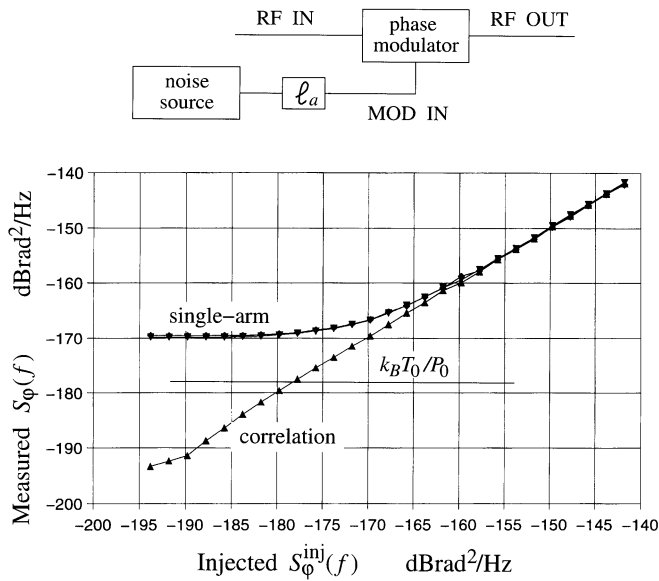


Fig. 6. Injection of phase noise in the DUT path.

A more conclusive experiment consists of the direct measurement of the S_ϕ floor in the presence of a small-angle phase modulation inserted in the DUT path, as shown in Fig. 6; the reported values are averaged around the Fourier frequency of 50 kHz. The phase modulator is driven by the internal noise source of the FFT analyzer, attenuated by a factor ℓ_a . As ℓ_a increases (leftwards in the figure), the injected noise S_ϕ^{inj} decreases proportionally to $1/\ell_a$. In the left part of the figure, for $S_\phi^{\text{inj}} < -160$ dBBrad²/Hz, the single-arm measures are limited by the amplifier noise. On the other hand, the correlation measures are well aligned on the straight line $S_\phi = S_\phi^{\text{inj}}$ even on the left part of the plot, where the injected signal is lower than the thermal floor $k_B T/P_0 \simeq -178$ dBBrad²/Hz.

V. REDUCTION OF THE RESIDUAL FLICKER NOISE

The scheme of Fig. 2 and the prototype described in the previous Section are not optimized for the low Fourier frequencies. Yet, it was only at the end of the experiments that the importance of high sensitivity at the lowest Fourier frequencies was recognized clearly, as the most interesting parametric noise phenomena tend to be of the flicker type.

Provided the carrier suppression is sufficient to prevent the amplifier from flickering, the residual flicker of the machine is chiefly the noise of the interferometer, which originates in the variable devices ℓ and γ' . Replacing them with by-step ones results in improved stability of the interferometer, and, therefore, lower residual flicker. Of course, the carrier suppression is impaired. This is corrected in the scheme of Fig. 7 by injecting a fine tuning signal at the output of the first stage of the amplifier. The game consists of preventing the first stage from flickering by choosing a high linearity amplifier with a small gain, while a certain amount of noise in the injection point can be tolerated. The scheme of Fig. 7 derives from a different study, focused on real-time measurements [14], in which correlation could not be used. The instrument, designed for the carrier frequency of 100 MHz, is a modified version of that described in the previous Section. The stability of the carrier nulling is improved, and a

80–90 dB rejection can be obtained for about one hour. In our circuit, the noise at the $\ell_c - \gamma_c$ output is attenuated by 26.9 dB, referred to the DUT output.

Fig. 8 shows the residual noise of the instrument, measured with $P_0 = 7.8$ dBm and with γ'' set for the detection of AM and PM noise. The low-frequency flicker is $S_\alpha(1 \text{ Hz}) = -161.2$ dB(V²/V²)/(Hz) and $S_\phi(1 \text{ Hz}) = -160.3$ (dBrad²)/(Hz). The improvement in $S_\alpha(1 \text{ Hz})$ and $S_\phi(1 \text{ Hz})$ upon the previous version is of some 10 dB, which is observed by temporarily replacing the by-step attenuator (ℓ in Fig. 7) with a continuous one. Fig. 8 also shows the cross spectrum density $S_{\alpha\phi}(f)$ of the residual noise. The white noise reduction is of some 12 dB, which is consistent with the value of 11.9 dB expected from the average in the absence of correlated noise; thus, the noise floor is expected to further decrease, increasing the measurement time. At low frequencies, correlation is still effective, and a noise reduction of some 8 dB is achieved at $f = 1$ Hz. While the first experiment was made detecting AM and PM noise, we observed that the residual flicker is almost unaffected by changing γ'' , which indicates that the 8-dB improvement is also achieved with the $\pm 45^\circ$ detection. Hence, the residual flicker of the instrument is $S_\phi(1 \text{ Hz}) = -168$ dBBrad²/Hz.

Finally, we wish to stress that no attempt has been made to post-process the measured spectra in order to hide the spectral lines due to the 50 Hz mains and to mechanical vibrations. The low level of these stray signals is due to the RF amplification prior to detecting and to the increased mechanical stability that derives from having removed all the continuously variable elements from the critical path.

VI. FURTHER DEVELOPMENTS

A. Measurement of Quartz Resonators

The $\pm 45^\circ$ detection has a relevant potential of usefulness for the measurement of the frequency flicker of quartz resonators, which is the parameter that limits the short-term frequency stability in oscillator applications. The frequency fluctuation $\Delta\nu$ of the resonator can be derived from the phase fluctuation ϕ measured at low Fourier frequencies, below the cutoff frequency $f_L = \nu_0/2Q$, where it holds that $\phi = \Delta\nu/2Q\nu_0$. A previous experience with high-stability HF resonators [15] proves that a sensitivity up to 10^{-14} (Allan deviation) can be achieved with a simple interferometer in favorable conditions. One of the major difficulties encountered at that time was to divide the flicker noise—clearly of parametric origin—from the background noise. The latter includes the instrument noise and the thermal noise inherent in the dissipative loss of the resonator. This difficulty can be solved with the $\pm 45^\circ$ detection. The feature of rejecting the thermal noise without relying upon temperature uniformity is a further relevant point. In fact, the temperature of the resonator must be set at the turning point of its frequency-to-temperature function. The turning point is usually in the 45–85 °C range, for it would be impractical to stabilize the whole interferometer at that temperature. In addition, it is often necessary to insert two resonators in the interferometer in order to get rid of the oscillator noise. Interestingly, the difference in the turning point may be of 3–4 K for a pair of devices

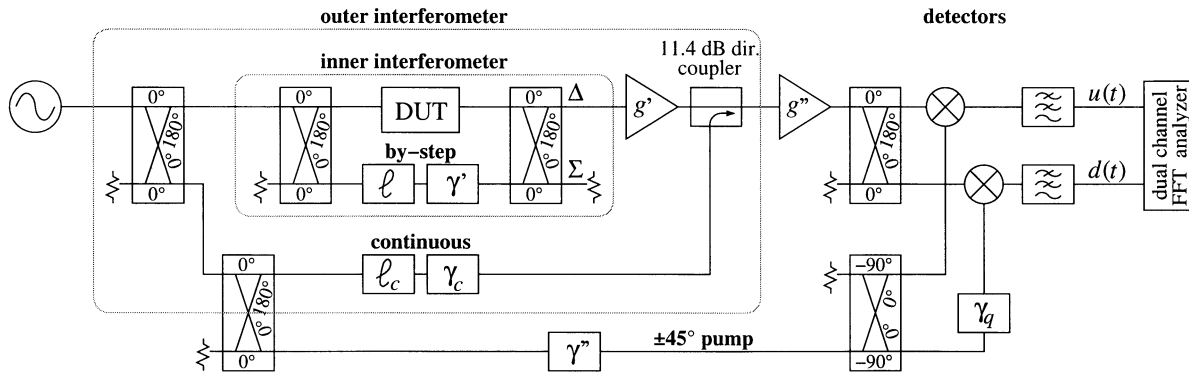


Fig. 7. Improved carrier suppression scheme.

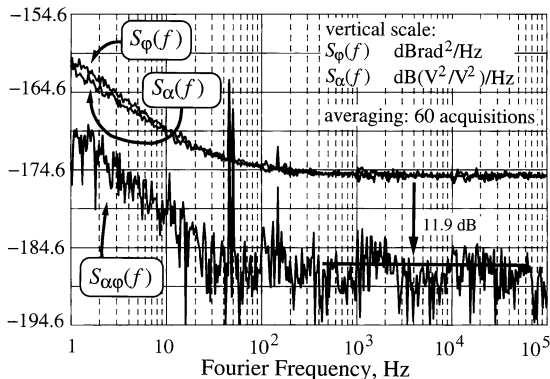


Fig. 8. Residual noise of the dual carrier suppression instrument, in the absence of the DUT.

nominally equal, but it can be of 30–40 K for a pair of resonators cut at different angles and otherwise similar.

B. Low-Frequency Applications to Solid-State Physics

The initial hypothesis on the AM and PM noise is reversed at audio frequencies and below. The AM noise is dominant at those frequencies, while too large capacitance fluctuations would otherwise be necessary to modulate the DUT phase. The $\pm 45^\circ$ detection was first used to measure the $1/f$ resistance fluctuations in thin metal films [6]; in this case, the $1/f$ signal to be detected is smaller than $k_B T_0$ at Fourier frequencies even lower than 1 Hz. A capacitive bridge was used to null the 2-kHz carrier, while the low film impedance had to be increased with a transformer; then, a commercial lock-in amplifier could be used as the $\pm 45^\circ$ detector, exploiting the internal phase offset facility.

Resistivity fluctuations caused by temperature-activated motion of lattice defects contribute the $1/f$ noise in thin metal films. Experiments were made aimed to identify some defect types, namely vacancies, self-interstitials, dislocations, and grain-boundaries [16], [17]. A review of these experiments is available in [18]. Studying the defects through their $1/f$ signature as a function of temperature, it is possible to calculate the distribution of the activation energies according to the Dutta-Dimon-Horn model [19].

Flicker noise also serves as an early indicator of electromigration damage in thin metal films, as it was studied on polycrystalline Aluminum and $\text{AlSi}_{0.01}\text{Cu}_{0.002}$ samples [20]. For example, in the $\text{AlSi}_{0.01}\text{Cu}_{0.002}$ alloy the peak of the activation energy distribution of the atomic motion occurs at 0.7 eV

TABLE I
COMPARISON BETWEEN PHASE NOISE MEASUREMENT METHODS

method	suitable to	residual noise dB[rad ²]/Hz 1/f white	references
saturated mixer	RT S_φ only	-145 -165	[22]
interferom.	RT S_φ, S_α	-150 -180	[4], [5]
dual carrier suppr. interf.	RT S_φ, S_α	-160 -180	[14]
dual satur. mixer	CA S_φ only	-150 -180	[22], [23]
double interferom.	CA S_φ, S_α	-155 -194	[13], [21]
$\pm 45^\circ$ interferom.	CA see Sec. I	-154 -190	Sec. IV
improv. $\pm 45^\circ$ interferom.	CA see Sec. I	-168 -190	Sec. V

RT = real-time, CA = correlation-and-averaging
1/f, refers to the 1 Hz coefficient

in the undamaged sample, which is due to the self-diffusion of Al atoms in strongly disordered grain-boundaries. The peak energy becomes 1.0 eV in the damaged sample, consistent with the Cu diffusivity along the Al grain-boundaries, which reveals that electromigration causes Cu atoms to drift and to be trapped at the grain-boundaries. Finally, we wish to stress that the flicker noise approach to study electromigration is preferable to the commonly used median time to failure (MTF) method because it makes use of one progressively damaged sample instead of requiring numerous destructive tests.

VII. CONCLUSION

The reader may be interested in extending the proposed experiments to other frequencies. No particular difficulty is expected in the range from less than 1 MHz to some 2 GHz, where almost all the building blocks we need are available and based on the same technology. Working in the microwave bands (2–40 GHz) requires some minor changes in technology, as Wilkinson power splitter and 90° hybrids are to be preferred. Our previous experiences indicate that a microwave implementation tends to be more straightforward than the corresponding HF-VHF one [5], while a sensitivity higher than $k_B T_0/P_0$ has been attained at 7.3 GHz [21].

Table I compares some methods for the measurement of phase noise and reports the residual noise in the HF-VHF applications. The saturated mixer instruments are easy to design and use,

and work in a wide frequency range; commercial implementations are available. The interferometer works properly even at low power (-30 dBm), out of reach for the saturated mixer; on the other hand, it generally needs to be designed for a specific frequency. Transforming an interferometer into the $\pm 45^\circ$ interferometer is a relatively simple task, as no change is needed in the low-noise part of the circuit; nonetheless, a dual-channel FFT analyzer becomes necessary. The dual carrier suppression schemes exhibit outstanding sensitivity at low Fourier frequencies, at the expense of increased complexity; some patience and skill may be needed to adjust the carrier rejection. The $\pm 45^\circ$ detection is expected to be particularly useful when parametric noise must be measured in the presence of a background of random noise, and when the temperature of the DUT can not be set arbitrarily.

REFERENCES

- [1] C. H. Horn, "A carrier suppression technique for measuring S/N and carrier/sideband ratios greater than 120 dB," in *Proc. 23rd Freq. Contr. Symp.*, Fort Monmouth, NJ, May 6–8, 1969, pp. 223–235.
- [2] K. H. Sann, "The measurement of near-carrier noise in microwave amplifiers," *IEEE Trans. Microwave Theory Tech.*, vol. 9, pp. 761–766, Sept. 1968.
- [3] F. Labaar, "New discriminator boosts phase noise testing," *Microwaves*, vol. 21, pp. 65–69, Mar. 1982.
- [4] E. N. Ivanov, M. E. Tobar, and R. A. Woode, "Microwave interferometry: application to precision measurements and noise reduction techniques," *IEEE Trans. Ultrason., Ferroelect. Freq. Contr.*, vol. 45, pp. 1526–1535, Nov. 1998.
- [5] E. Rubiola, V. Giordano, and J. Gros Lambert, "Very high frequency and microwave interferometric PM and AM noise measurements," *Rev. Sci. Instrum.*, vol. 70, pp. 220–225, Jan. 1999.
- [6] A. H. Verbruggen, H. Stoll, K. Heeck, and R. H. Koch, "A novel technique for measuring resistance fluctuations independently of background noise," *Appl. Phys. A*, vol. 48, pp. 233–236, Mar. 1989.
- [7] B. P. Kibble and G. H. Rayner, *Coaxial AC Bridges*. Bristol, U.K.: Adam Hilger, 1984.
- [8] P. Osváth, "Measurement of impedances," in *Technology of Electrical Measurements*, L. Schnell, Ed. Chichester, U.K.: Wiley, 1983, pp. 147–223.
- [9] L. Meade, *Lock-In Amplifiers: Principle and Applications*: IEE, 1983.
- [10] "Broadcasting Service (Television)," International Telecommunication Union (ITU), Geneva, Switzerland, report no. 624-3, pt. 1, vol. XI, Recommendations and Reports of the CCIR, 1986.
- [11] S. O. Rice, "Mathematical analysis of random noise (part I and II)," *Bell Syst. Tech. J.*, vol. 23, pp. 282–332, July 1944.
- [12] C. M. Allred, "A precision noise spectral density comparator," *J. Res. NBS*, vol. 66C, pp. 323–330, Oct.–Dec. 1962.
- [13] E. Rubiola and V. Giordano, "Correlation-based phase noise measurements," *Rev. Sci. Instrum.*, vol. 71, pp. 3085–3091, Aug. 2000.
- [14] —, "Dual carrier suppression interferometer for the measurement of phase noise," *Electron. Lett.*, vol. 36, pp. 2073–2075, Dec. 7, 2000.
- [15] E. Rubiola, J. Gros Lambert, M. Brunet, and V. Giordano, "Flicker noise measurement of HF quartz resonators," *IEEE Trans. Ultrason., Ferroelect. Freq. Contr.*, vol. 47, pp. 361–368, Mar. 2000.
- [16] J. Briggmann, K. Dagge, W. Frank, A. Seeger, H. Stoll, and A. H. Verbruggen, "Irradiation-induced defects in thin aluminum films studied by $1/f$ noise," *Phys. Status Solidi (A)*, vol. 146, pp. 325–335, Nov. 1994.
- [17] M. J. C. van den Homberg, A. H. Verbruggen, P. F. A. Alkemade, S. Radelaar, E. Ochs, K. Armbruster, A. Seeger, and H. Stoll, " $1/f$ noise in mono- and polycrystalline aluminum," *Phys. Rev. B*, vol. 57, pp. 53–55, Jan. 1998.
- [18] A. Seeger and H. Stoll, " $1/f$ noise and defects in thin metal films," in *Proc. 15th Int. Conf. Noise Phys. Syst. 1/f Noise*, C. Surya, Ed., Hong Kong, Aug. 23–26th, 1999, pp. 162–167.
- [19] P. Dutta, P. Dimon, and P. M. Horn, "Energy scales for noise processes in metals," *Phys. Rev. Lett.*, vol. 43, pp. 646–649, Aug. 1979.
- [20] C. A. Kruelle, E. Ochs, H. Stoll, A. Seeger, and I. Bloom, "Electromigration damage in aluminum alloys studied by $1/f$ noise," in *Proc. Mater. Reliability Microelectron. VIII Symp.*, vol. 516, Matrial Research Society Proceedings, J. C. Bravman, T. N. Marieb, J. R. Lloyd, M. A. Korhonen, and P. A. Warrendale, Eds., San Francisco, CA, Apr. 13–16th, 1998, pp. 3–8.
- [21] E. Rubiola, V. Giordano, and J. Gros Lambert, "Improved interferometric method to measure near-carrier AM and PM noise," *IEEE Trans. Instrum. Meas.*, vol. 48, pp. 642–646, Apr. 1999.
- [22] Chronos group, *Frequency Measurement and Control*. London, U.K.: Chapman & Hall, 1994.
- [23] W. F. Walls, "Cross-correlation phase noise measurements," in *Proc. 46th Freq. Contr. Symp.*, New York, May 27–29, 1992, pp. 257–261.



Enrico Rubiola was born in Torino, Italy, in 1957. He received the Ph.D. degree metrology from the Italian Ministry of Scientific Research, Rome, Italy, in 1988.

After having been a Researcher at the Politecnico di Torino and a Professor at the University of Parma, Parma, Italy, he is now a Professor within the Université Henri Poincaré (UHP), Nancy, France. He is a researcher at the Laboratory of Physics of Ionized Media and Applications (LPMIA), UHP. He teaches electronics at the Ecole Supérieure de Sciences et

Technologies de l'Ingénieur de Nancy (ESSTIN), the state engineering school within the UHP, where he is also in charge of the Department of Electronics. He has worked on various topics in electronics and metrology, namely navigation systems, time and frequency comparisons, atomic frequency standards, and gravity. His main fields of interest are precision electronics and phase noise metrology, which include frequency synthesis, high spectral purity oscillators, and noise.



Vincent Giordano was born in Besançon, France, on February 20, 1962. He received the engineer degree in 1984 from the Ecole Supérieure de Mécanique et des Microtechniques, Besançon, France, and the Ph.D. degree in physical sciences in 1987 from the Paris XI University, Orsay, France.

From 1984 to 1993, he was a researcher of the permanent staff of the Laboratoire de l'Horloge Atomique, Orsay, France, where he worked on a laser diode optically pumped cesium beam frequency standard. In 1993, he joined the Laboratoire de Physique et de

Métrologie des Oscillateurs (LPMO), Besançon, where he is the Head of the Microwave Metrology team. Presently, his main area of interest is the study of high spectral purity microwave oscillators and the high sensibility phase noise measurement systems.



Hermann Stoll received the diploma degree and the Ph.D. degree in physics from the Stuttgart University, Stuttgart, Germany, in 1976 and 1981, respectively. His thesis, under the supervision of Prof. Dr. A. Seeger, investigated vacancy-induced noise in thin metal films.

He has performed measurements at the Max-Planck-Institute for Metal Research, Stuttgart, and at the National Electrotechnical Institute, Torino, Italy. Since 1981, he has been with the Max-Planck-Institute for Metal Research. He has expanded his research on defect-induced resistance fluctuations ($1/f$ noise) to the diffusion of defects in dislocations and grain boundaries, and to quantitative studies of electromigration-damage in Aland Cu interconnects. He has been involved in the construction of novel MeV positron (e^+) beams and the development of the age-momentum-correlation (A MOO) techniques. The latter was applied to the study of defects in metals, semiconductors, and polymers, and to the formation and chemical reactions of positronium (positronium; chemistry). He has published numerous papers on these subjects.